表2　参加施設（五十音順）

神奈川県立足柄上病院
神奈川県立がんセンター
恵生会上白根病院
国家公務員共済組合連合会平塚共済病院
国家公務員共済組合連合会横浜南共済病院
済生会横浜市南部病院
総合病院秦野赤十字病院
同友会藤沢湘南台病院
三浦市立病院
横浜市立大学付属病院（第一外科）

表3　患者背景

原発部位	結腸癌	6例	初発／再発	
	直腸癌	11例	初発	13例
			再発	4例
性別	男性	12例		
	女性	5例	評価病変	
			肝転移	10例
平均年令		61.6才	肺転移	6例
		(40～74才)	リンパ節転移	2例
			骨盤内転移	2例
PS	0	17例		
	1	0例		

表4　抗腫瘍効果

CR	PR	SD	PD	奏効率
0例	3例	12例	2例	17.6%（3/17）

RECIST 評価

PR：肝転移　2例　　PD：肝転移　1例
　　肺転移　1例　　　　肝＋骨盤内病変　1例

Disease-control rate（CR+PR+SD）　88.2%

投与コース中央値　8コース（継続中5例含む）

表5　有害事象　(CTCAE Ver3.0)

	Grade					
	1	2	3	4	計	Grade3/4
白血球減少	0	3	4	0	7(41.2%)	4(23.5%)
好中球減少	2	0	2	0	4(23.5%)	2(11.8%)
悪心	1	0	0	0	1(5.9%)	0
嘔吐	0	1	0	0	1(5.9%)	0
食思不振	0	1	0	0	1(5.9%)	0
口内炎	0	1	0	0	1(5.9%)	0
下痢	0	1	0	0	1(5.9%)	0
味覚障害	0	1	0	0	1(5.9%)	0
吃逆	1	0	0	0	1(5.9%)	0
発疹	1	0	0	0	1(5.9%)	0
肝機能障害	1	0	0	0	1(5.9%)	0
末梢神経障害	0	1	0	0	1(5.9%)	0

PS：0，主病変は結腸癌6例，直腸癌11例，stage Ⅳの初発例が13例，再発例が4例，評価可能病変として肝転移10例，肺転移6例，リンパ節2例，骨盤内病変2例であった．

2　抗腫瘍効果（表4）

プロトコール治療のコース数は，継続中を含めて中央値8コースであった．抗腫瘍効果はCR：0例，PR：3例，SD：12例，PD：2例の結果であり，奏効率は17.6%(3/17)であった．PRとなった3例は，4コース，6コース，7コースの時点でPRとなっており，評価病変は肝転移2例，肺転移1例であった．PR3例とSD12例をあわせたDisease-control rate（腫瘍増殖抑制率）は88.2%であった．一方，PDとなった2症例は肝転移例と肝＋骨盤内病変例であった．

3　有害事象（表5）

血液毒性としての有害事象は，白血球減少7例(41.2%)，好中球減少4例（23.5%）に認めており，Grade3/4はそれぞれ4例（23.5%），2例（11.8%）に認め，そのほとんどが4コースまでに初回発現していた．消化器症状としての食思不振，悪心，嘔吐，下痢，口内炎，味覚障害は，Grade1/2のものを各1例（5.9%）に認めたが，そのほとんどが血液毒性同様4コースまでに初回発現しており，対処により治療継続可能な程度であった．また，肝機能障害（Grade1）1例，末梢神経障害1例を認めている．

4　転帰，後療法

解析時点での生存例は13例で，本療法継続中が5例である．死亡例4例は全例原病死であった．後療法としてFOLFOX療法が施行された症例は9例，経口抗癌剤投与1例，無治療2例であった．

考　察

大腸癌に対する化学療法は，1957年にHeidelberger[9]によって開発された5FUを基本とした治療が現在でも続けられている．これまでに様々な工夫を行いながら施行されてきて居り，Mitomycin，Vincristineなどの抗癌剤との併用療法も試みられてきたが十分な効果を得ることはできなかった．1980年代になりbest supportive careに対する化学療法の明らかな有用性がエビデンスとして示され[10]，さらに1990年代にはBiochemical modulation (BM)[11]の考えに基づいた治療へと発展していった．併用薬剤としてMethotrexate (MTX)[12]，Levamisole (Lev)[13]，Leucovorin (LV)などが用いられたが，LV併用療法が抗腫瘍効果，延命効果ともに優れているとされ[14]，以後5FU/LV療法が標準とされるに至っている．5FU/LV療法といっても5FUの投与方法には差異があり，bolus投与のRosewell Park Memorial Institute (RPMI) regimen[1]，Mayo regimen[15]と持続投与のde Gramont regimen (LVFU2)[2]，AIO regimen[16]が存在した．これら

の治療方法は，RPMI regimen が1999年に，LVFU2 は2005年1月に我が国で遅ればせながら認可されているが，CPT-11との併用療法としては明示されていない．

我が国では，経口抗癌剤の開発が厳格な RCT が行われないまま化学療法の中心に存在してきたことが，欧米での化学療法の発展とは期を同じくしなかったと思われる．CPT-11と L-OHP はほぼ同時期に大腸癌に対する検証が進められている．1998年 Cunningham ら[3]により CPT-11単剤での有用性が，2000年には Saltz ら[4]による IFL 療法（CPT-11/bolus5FU/LV）の有用性が奏効率39%，MST 14.8ヶ月と報告され，Duillard ら[5]による FOLFIRI 療法（CPT-11/infusional5FU/LV）では奏効率49%，MST17.4ヶ月と報告されている．一方，L-OHP については2000年に de Gramont regimen（LVFU2）との併用による FOLFOX4[6]での有用性が報告され，奏効率50.7%，progression-free survival 9.0ヶ月とされた．さらに2004年 Tournigand ら[17]により FOLFIRI，FOLFOX6 の reverse sequence study が報告され，FOLFIRI 先行群，FOLFOX 先行群の両群の有用性は同等であると報告された．L-OHP は我が国では2005年3月に認可されている．

このような環境の中，我々は2004年に CPT-11併用5FU/l-LV 療法実施計画を臨床試験として作成し12月より登録開始とした．5FU/LV 療法の選択については，5FU/l-LV 療法の検討時[18]には RPMI regimen にて施行したが，本試験では infusional 5FU 療法の方が優れているとの判断から infusional 5FU 療法を選択し，多施設共同研究であることを考慮し，簡便さと外来での治療が施行可能な点を加味して sLVFU2 を選択した．また，開始時の各施設での本療法施行例数は少なく，5FU 投与量は FOLFIRI 療法と同じく bolus5FU 400mg/㎡，infusion5FU 2400mg/㎡と設定したが，CPT-11の投与量については，安全性を最優先に考慮し小松ら[19]が進行大腸癌に関して報告している CPT-11併用5 FU/l-LV 療法の CPT-11の投与量100mg/㎡を採用した．

今回の検討は，登録症例数が予定数の約半数となった時点（2006年1月）での解析である．

解析対象症例17例の検討では，PR 3例を認めたのみで17.6%の奏効率であった．この結果は，IFL 療法や FOLFIRI 療法に遠く及ばず，LVFU2 療法より下回った成績となって居り，CPT の上乗せ効果は全く認められなかった．Dose intensity の面からみると，4コースまでは CPT 91.9%，bolus5FU 92.2%，infusion5FU 91.2%と効果が期待できる用量と思われるが，5－8コースではそれぞれ82.5%，79.7%，79.0%と低下して居り，9コース以降ではさらに低下していた．今回の結果では，PR を示した3例は4コース，6コース，7コースの時点であり，Tournigand らの報告では Response の中央値は2.1ヶ月であるので，4コースまでの Dose intensity から考えればもう少し良い結果が得られるものと思われた．以上の結果から，5FU の投与量を bolus400mg/㎡は FOLFIRI 療法と同じであるが，infusion2400mg/㎡は FOLFIRI 療法での infusion2400－3000mg/㎡の下限に設定した点と CPT-11を100mg/㎡に設定した点が奏効率の低下の原因と判断した．特に CPT-11については奏効率の面からは投与量100mg/㎡では不十分であり，有害事象の発生を考慮すれば併用しない方が良いとも考えられた．

一方，PR 3例と SD12例をあわせた Disease-control rate（腫瘍増殖抑制率）は88.2%と比較的良い結果であり，中間解析のために観察期間が短かく参考値ではあるが，Progession-Free Survival（Kaplan-Meier 法）は6.5ヶ月であった．Tumor dormancy の観点からは一考に値するかも知れない．

有害事象についてみてみると，de Gramont らの LVFU2 療法での報告では，好中球減少11.5%（Grade3/4：1.9%），下痢31.3%（G3/4：2.9%），嘔気42.4%（G3/4：3.9%），口内炎22.1%（G3/4：1.9%）であり，Saltz らの IFL 療法では，白血球減少 G3/4：8.9%，下痢 G3/4：22.7%，嘔吐 G3/4：9.7%，口内炎 G3/4：2.2%，Duillard らの FOLFIRI 療法では，白血球減少74.1%（G3/4：20.4%），好中球減少71.2%（G3/4：28.8%），下痢88.9%（G3/4：44.4%），嘔吐55.6%（G3/4：11.1%），食思不振29.6%（G3/4：7.4%），口内炎25.9%（G3/4：0%）と報告されている．本試験では，有害事象は，全体を通して白血球減少7例（41.2%），好中球減少4例（23.5%）と血液毒性が顕著であったが，Grade3/4はそれぞれ4例（23.5%），2例（11.8%）に認め，そのほとんどが4コースまでに初回発現している．白血球，好中球減少の発生は LVFU2 療法より明らかに高率で，FOLFIRI 療法と同率であった．その他に消化器症状としての食思不振，悪心，嘔吐，下痢，口内炎，味覚障害は，Grade1/2のものを各1例（5.9%）に認めたが，その発生率の比較ではるかに低率であり，そのほとんどが血液毒性同様4コースまでに初回発現して居り治療継続には支障をきたさない程度であった．また，肝機能障害（Grade 1）1例，末梢神経障害1例を認めているが，休薬により改善している．

以上の中間解析の結果，本臨床試験では 5FU/l-LV 療法に CPT-11併用することによる抗腫瘍効果の増強は認められなかったこと，安全に施行可能であったが，有害事象としての血液毒性は 5FU/LV 療法より高率であったことが明らかとなった．したがって，本臨床試験は中止する方針とし新たな治療計画を作成することとした．今後の CPT-11の投与量は，我が国での承認用量を考慮すると150mg/㎡が推奨用量と想定される．

Abstract

COMBINATION THERAPY WITH IRINOTECAN, FLUOROURACIL, AND l-LEUCOVORIN IN PATIENTS WITH METASTATIC COLORECTAL CANCER

Makoto AKAIKE, Yuji YAMAMOTO, Makoto TAKAHASHI, Ryuji SHIRAISHI, Hiroshi MATSUKAWA, Tatsuo MAKINO, Hiroharu SUZUKI, Isao TAMURA, Yukihiro OZAWA, Yasushi RINO
Kanagawa Colorectal Cancer Study Group

Object: As a project of the Kanagawa Colorectal Cancer Study Group we studied the efficacy of using a combination of irinotecan (CPT-11), fluorouracil (FU), and l-leucovorin (l-LV) to treat metastatic colorectal cancer.

Patients and Methods: We treated PS 0-1 patients with measurable or assessable colorectal cancer who either had not received preliminary treatment, or were postoperative with metastasis and had undergone radiation therapy or adjuvant chemotherapy before more than 4 weeks, and further had provided written acceptance of our proposed procedures. The treatment consisted of adding CPT-11 to the basic sLV5FU2 treatment. The amounts used per square meter of body surface were 2400 mg 5FU as an infusion and 400 mg 5FU as a bolus, plus 200 mg l-LV and 100 mg CPT-11. Tumor response was assessed by RECIST and toxicity by NCI-CTC.

Results: 17 patients meeting our criteria underwent an average of 8 courses of treatment. Objective tumor response rate was 17.6%, and disease-control rate was 88.2%. Regarding hematologic toxicity, 7 patients (41.2%) experienced leukopenia, which developed to grade 3/4 in 4 (23.5%) of them. Another 4 patients experienced neutropenia (23.5%), which developed to grade 3/4 in 2 (11.8%) of them. Digestive toxic effects were observed in 5.9% of the patients.

Conclusion: This clinical study was safely carried out, but median analysis did not show that the combination of FU and l-LV with CPT-11 increased antitumor efficiency. A probable reason for this is that the dose of CPT-11 was insufficient.

Abstract

COMBINATION THERAPY WITH IRINOTECAN, FLUOROURACIL, AND l-LEUCOVORIN IN PATIENTS WITH METASTATIC COLORECTAL CANCER

Makoto AKAIKE, Yuji YAMAMOTO, Makoto TAKAHASHI, Ryuji SHIRAISHI, Hiroshi MATSUKAWA, Tatsuo MAKINO, Hiroharu SUZUKI, Isao TAMURA, Yukihiro OZAWA, Yasushi RINO
Kanagawa Colorectal Cancer Study Group

Object: As a project of the Kanagawa Colorectal Cancer Study Group we studied the efficacy of using a combination of irinotecan (CPT-11), fluorouracil (FU), and l-leucovorin (l-LV) to treat metastatic colorectal cancer.

Patients and Methods: We treated PS 0-1 patients with measurable or assessable colorectal cancer who either had not received preliminary treatment, or were postoperative with metastasis and had undergone radiation therapy or adjuvant chemotherapy before more than 4 weeks, and further had provided written acceptance of our proposed procedures. The treatment consisted of adding CPT-11 to the basic sLV5FU2 treatment. The amounts used per square meter of body surface were 2400 mg 5FU as an infusion and 400 mg 5FU as a bolus, plus 200 mg l-LV and 100 mg CPT-11. Tumor response was assessed by RECIST and toxicity by NCI-CTC.

Results: 17 patients meeting our criteria underwent an average of 8 courses of treatment. Objective tumor response rate was 17.6%, and disease-control rate was 88.2%. Regarding hematologic toxicity, 7 patients (41.2%) experienced leukopenia, which developed to grade 3/4 in 4 (23.5%) of them. Another 4 patients experienced neutropenia (23.5%), which developed to grade 3/4 in 2 (11.8%) of them. Digestive toxic effects were observed in 5.9% of the patients.

Conclusion: This clinical study was safely carried out, but median analysis did not show that the combination of FU and l-LV with CPT-11 increased antitumor efficiency. A probable reason for this is that the dose of CPT-11 was insufficient.

特集 Stage IV 大腸癌と診断したらどうするか

肺転移を伴う stage IV 大腸癌の治療方針

Surgical strategy for the treatment for stage IV colorectal cancer with pulmonary metastases

大植 雅之[*2] OHUE Masayuki
東山 聖彦[*5] HIGASHIYAMA Masahiko
尾田 一之[*4] ODA Kazuyuki
能浦 真吾[*1] NOURA Shingo
岡見 次郎[*4] OKAMI Jiro
前田 純[*4] MAEDA Jun
矢野 雅彦[*3] YANO Masahiko
児玉 憲[*7] KODAMA Ken
石川 治[*6] ISHIKAWA Osamu
今岡 真義[*8] IMAOKA Shingi

当施設において1981～2006年までに149例の大腸癌肺転移に対する初回肺切除を経験し，全体の3年生存率66.9%，5年生存率51.9%，10年生存率40.7%，中央生存期間は5年9ヵ月であった．とくに，肺転移巣に限った胸部所見(胸部CT)では，①縦隔リンパ節腫大がなく，②転移個数が2個まで，③悪性胸水，播腫がない症例では，積極的適応として外科切除を行い，5生率61%と良好な成績を上げている．一方，これら149例中，肺転移を伴うstage IV大腸癌(同時性肺転移症例)は12例(8.1%)で，肺単独転移8例，肺肝転移4例であった．症例数は少ないものの，肺単独転移例の5年生存率は83.3%で，肺肝転移例の3年生存率は25.0%であった．肺転移を伴うstage IV大腸癌に対しては原発巣，転移巣ともに外科的切除が原則とされているが，とくに肺孤立性転移症例では長期生存例がみられるため，良好な適応と考えられる．一方，他臓器転移(主に肝転移)例や肺転移個数が複数である症例では，その治療選択は慎重に行う必要がある．

はじめに

大腸癌26,091人の同時性遠隔転移頻度は，肝10.7%，腹膜5.0%，肺1.6%，骨0.3%と報告されており[1]，Stage IVの遠隔臓器として肺は3番目に多いことになる．肺転移を伴うStageIV大腸癌症例で，原発巣に対する外科切除の機会は少なくないが，肺転移巣に対する外科治療は比較的まれである．したがって，大腸癌肺転移巣に対する手術成績は大半を占める異時性肺転移症例の成績を反映していることが多く，同時性肺転移症例に限った肺切除の適応，成績と意義はいまだ明確ではない．

大阪府立成人病センター *1消化器外科 *2同副部長 *3同部長 *4呼吸器外科 *5同部長 *6同センター院長 *7同センター副院長 *8同センター総長
Key words：大腸癌／Stage IV／肺転移／治療方針

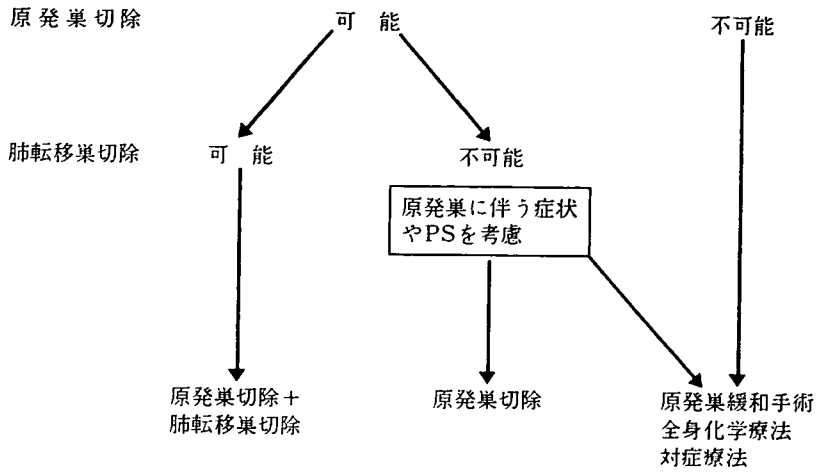

図1　肺転移を伴うstage IV大腸癌の治療方針(文献1より一部改変)

従来の一般的な転移性肺腫瘍に対する外科治療の適応は，1965年にThomfordらが報告したように，①耐術能があること，②原発巣がコントロールされていること，③肺以外に遠隔転移再発がないこと，④肺転移が一側肺であることの，4つの基準が引用されている[2]．その中でも大腸癌肺転移の外科成績は比較的良好で，近年の手術手技や器具，術後管理，化学療法などの進歩に伴い，肺転移切後の3年生存率は30～60%と報告されている[3)-5)]．また，2001年の第55回大腸癌研究会(主題Ⅰ：大腸癌肺転移のすべて)でアンケート調査が行われ，わが国の主要な79施設から回答を得た結果，肺転移切除例569例の5年生存率は38.8%，中央生存期間は39.2ヵ月，肺転移非切除例416例の5年生存率は2.4%，中央生存期間は14.4ヵ月と報告され，肺切除は明らかに有効な治療法であることが示されている[6]．すなわち，大腸癌ではThomfordらの適応のうち，④はすでに基準から外され，②③に関してもその制御が可能と判断すれば適応拡大が試みられようとしている．

同時性肺転移症例は，②の項目(さらに③も加わりうる)に対する積極的な適応拡大と考えられる．実際，すでに“肺転移を伴うstage IV大腸癌の治療方針”について，大腸癌治療ガイドラインでは原発巣，転移巣ともに切除可能であれば切除すると明記されている(図1)[1]．

今回，当施設で経験した同時性肺転移症例に対する肺切除症例の治療成績を示すとともに，その治療戦略に関する最近の知見を加えて述べる．

I. 術前診断

当施設では大腸癌の術前検査として，肺転移の発見目的に胸部単純X線に加えてヘリカルCTスキャンによるスクリーニングを行っている．画像上肺転移が疑われる陰影を発見したときには，造影CTにより縦隔リンパ節転移の有無なども含めて精査を行う．孤立性陰影では，原発性肺癌との鑑別はthin-sectionによる高分解能CTでおおむね鑑別が可能であるが，困難な時には気管支鏡検査などにて生検組織診や細胞診を行う．多発肺陰影では，CTにてその個数を確認するが，まれながら原発性肺癌も含まれている場合があり，その陰影の性状にも注意を払う[7]．また，CTの高い分解能のために数mmの小陰影が指摘され，肺転移か，原発性肺癌か，炎症性結節かの質的鑑別が困難な際には，原発巣の切除を優先し，肺の陰影については少なくとも3～4ヵ月の経過後，再度胸部CTを撮り肺病変に対する手術適応を決定すべきである．

II. 大腸癌肺転移巣に対する外科治療

ここでは，まず大腸癌肺転移巣に対するわれわ

れの施設における外科治療の基本的な適応・手技(原発巣との同時性肺転移症例には限らない)の概略を述べる.

大腸癌肺転移巣に対する胸部領域のみに限定した手術適応は,積極的適応と妥協的適応の2つに大きく分けている[8]. 前者は,胸部CTで,①縦隔リンパ節の転移を疑わせる腫大がない,②肺転移巣が2個まで,③悪性胸水や播種がない,である. 一方,後者は,①所属リンパ節転移を認める,②肺転移巣が4～6個までとし,さらに多発肺転移では,その左右別,表在性・深在性,肺葉上・中・下別など,その分布を考慮して手術適応と術式を決めている. とくに左右両側性の場合には,病態と手術侵襲程度より,開胸アプローチ法や,一期か二期手術かを決めるべきである.

術式は,肺部分切除・区域切除を基本としているが,腫瘍径が3cmを越えたり,2～3cmでも肺門に近い場合や原発性肺がんとの鑑別が困難な場合には肺門リンパ節の転移のサンプリングを兼ねた肺葉切除が選択される. 多発肺転移では,それら転移巣の分布と手術侵襲(とくに肺機能)を考慮した術式を選ぶ. 近年は胸腔鏡による肺切除術が普及し低侵襲の利点が報告されているが,肺切除マージンの確保,局所散布,微小転移の遺残などの問題点もあり,本手技は慎重に行われるべきである.

さらに当施設では大腸癌肺転移巣手術時に以下の工夫を行っている. 潜在的な胸膜播種を検出するために,開胸時には胸腔内洗浄細胞診(PLC)を施行している. PLC陽性例の予後は不良である. また,肺転移巣の周囲には娘結節を伴うことがしばしば経験され,しかも切除マージンが不十分であると断端再発を招くことになる. この様な術後再発を防止するため,術中肺切離面迅速細胞診を行っている. すなわち図2に示すように,肺切除時に使用した自動縫合切離器の使用後のカートリッジを生食水で洗浄し,その洗浄液の細胞診を術中迅速診断し,肺切除マージンが十分であるか(完全切除できているか)を確認する方法である[9]. 本手技で今までに約10%の細胞診陽性を経験しており,陽性例では追加切除を行っている. また切離マージンを一定に確保するために,自動縫合切離器よりNd：YAGレーザーや電気メスを用いて肺切離することもある.

このような適応や手技の工夫の結果,当施設では1981～2006年までに149例の大腸癌肺転移に対する初回肺切除を経験し,全体の3年生存率66.9%,5年生存率51.9%,10年生存率40.7%,中央生存期間は5年9ヵ月であった(図3). そのうち,積極適応症例の成績は5生率61%と良好であ

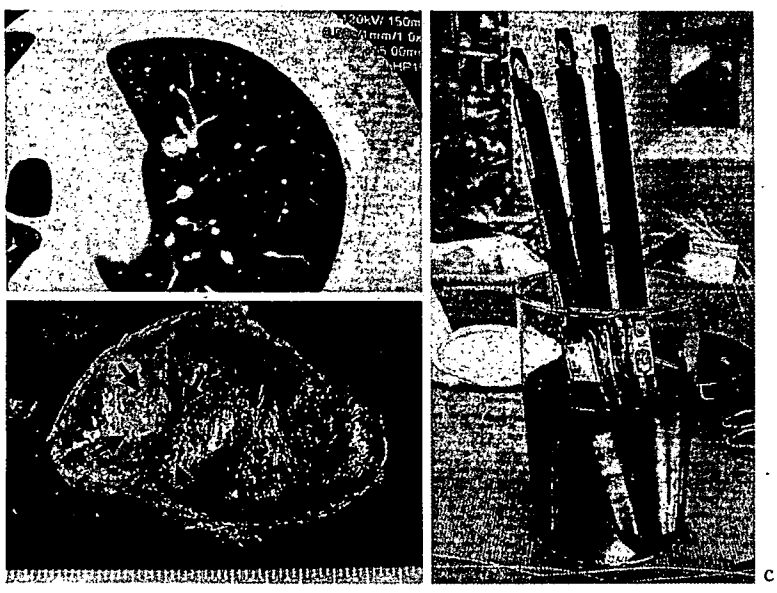

図2 大腸癌肺転移に対する肺部分切除時の肺切離面洗浄細胞診

左肺上葉の孤立性転移巣対し(a),肺部分切除を行った(b：腫瘍矢印). その際,使用した自動縫合切離器のステイプルカートリッジを生食水にて洗浄し(c),洗浄液を細胞診として提出,肺切離面細胞診陰性を術中に確認する.

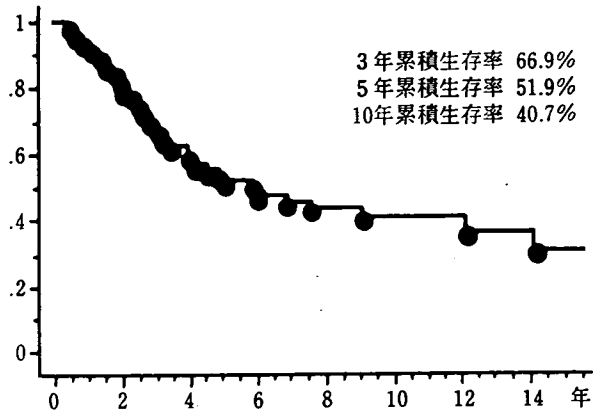

図3 大腸癌肺転移(149例)の初回肺切除からの長期累積生存率

った.

III. 当センターにおける同時性手術症例と成績

StageIV の症例では Stage II, III 症例に比べて生物学的に悪性度が高く，原発巣における癌の浸潤やリンパ節転移が高度であることも多いので，まずは原発巣の切除を先行し局所の根治性を評価する必要がある．また，原発巣と転移巣が異なる体腔内にあるために，大腸癌肝転移とは異なり同時性肺転移症例でも異時切除となることが多い．表1に当施設で経験した大腸癌 Stage IV 肺転移切除12例(症例番号は年次順)を示した．肺切除時平均年齢は62.5歳，男性8例，女性4例である．原発巣には根治手術がなされており，結腸が8例と多く，肺転移8例に加えて肺肝転移は4例であった．当初は肺孤立性転移のみであったが，時代の変遷とともに肺両側多発や肺肝転移も切除の対象となっている．他院で原発巣手術を行った3例を除く9例中4例は1期的手術であり，いずれも肺転移は1個である．また，肺肝転移4例中3例は2期的切除であるが，腹腔内の病巣はいずれも1期的に切除されている．最近では両側肺転移を2期的切除としている，などの傾向がある．初再発部位は，残肺，肝，大動脈リンパ節などで，再発した5例中3例に再発巣切除が行われ，うち1例(症例5)では再々発を認めず，他癌死したものの長期生存に至っている．肺孤立性転移の2例(症例3，4)は10年以上の無再発長期生存である．全体では症例が少ないものの，図4に示すように肺単独転移例の5年生存率は83.3%で，肺肝転移例の3年生存率は25.0%であった．

文献的には，DFI が有意な予後規定因子であるという報告もみられ[5)6)]，同時性肺転移が異時性肺転移と比較して予後が不良であるとされているが，われわれの検討では両者に有意差は認めなかった．また，制御可能な肝転移例における肺切除の有用性の報告[10)-12)]や，肺切除後の残肺再発に対する再肺切除の有用性の報告[13)]もなされている

表1 Stage IV 同時性肺転移大腸癌(12例)

症例	年/性	原発	リンパ節転移個数	転移部位と個数	肺切除までの日数	手術回数	再発	再発巣切除	再々発	観察期間	転帰
1	60代 M	結腸	NA	肺 1	124	2	無			3年	他病死
2	50代 F	結腸	0	肺 1	0	1	無			2年2月	生存
3[a]	50代 F	直腸	NA	肺 1	181	2	無			13年8月	生存
4	50代 F	結腸	0	肺 1	0	1	無			15年11月	生存
5	60代 M	結腸	1	肺 2	58	2	肝	有	無	12年2月	他癌死
6[a]	60代 M	結腸	0	肺 2 肝 2	177	2	肺肝	有	肺肝	2年2月	原癌死
7	50代 F	直腸	34	肺両 2 肝 1	16	2	N4[c]	無		1年6月	原癌死
8	50代 M	結腸	2	肺 3 肝 1	30	2	肺	無		3年10月	担癌生存
9	70代 M	結腸	1	肺 1 肝 1	0	1	肺	有	小脳[d]	2年7月	原癌死
10	70代 M	直腸	0	肺 1	0	1	無			3年11月	生存
11	70代 M	結腸	0	肺両 5[b]	25	2	無			8月	生存
12[a]	50代 M	直腸	NA	肺両 2[b]	56	3	無			3年8月	生存

a：原発巣手術は他院　b：両側肺転移に対して2期的肺切除　c：大動脈リンパ節　d：小脳転移巣切除

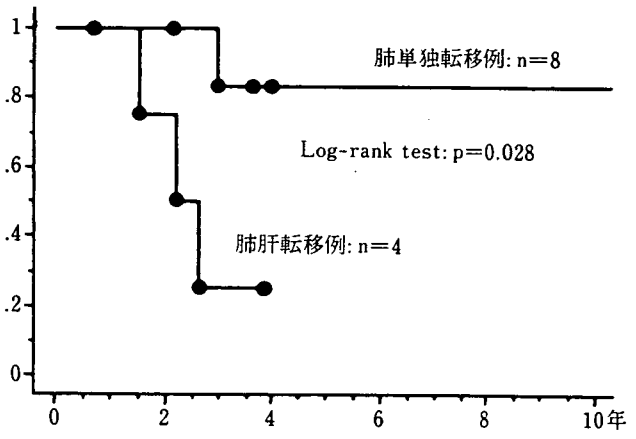

図4 肺転移を伴うStage IV大腸癌に対する外科治療成績

が，stage IV大腸癌についてのデータは少なく今後の検討課題である．

IV. 予後因子

一般的な大腸癌肺転移術後の5年生存率は30～60%と報告によりかなりの差がある[3)-5)]．この要因として，単一施設から症例数が100例を超える報告は少なく肺転移手術自体が少ないこと，各施設間の手術適応が異なることなどがあげられる．われわれは肺切除の適応を積極的適応と妥協的適応に分けているが，肺転移の予後因子についてはいまだに十分なコンセンサスは得られていない．また，とくに今回のテーマである同時性肺転移例は異時性に比較して手術の対象となる症例が少なく，今後，多施設間で症例を集積するとともにさまざまな予後因子を解析(＝良好な手術適応基準の決定)する必要がある．現在までによく検討されている大腸癌肺転移(主に異時性肺転移例)の予後因子を表2に列挙した[4)-6)14)]．大腸癌取扱い規約(第7版)では，肝転移症例のGradeに原発巣のリンパ節転移の程度が加味されているが[1)]，肺転移症例でも検討に値すると思われる．

V. その他の肺転移巣に対する治療

1. 化学療法

最近ではわが国でも新規抗癌剤を併用したFOLFOX(infusional 5-FU/LV/oxaliplatin)やFOLFIRI(infusional 5-FU/LV/irinotecan)が日常臨床で積極的に用いられるようになってきた[15)16)]．欧米では40%を超える高い奏効率や2年以上の生存期間延長がすでに報告されているが，肺転移切除不能例においても同様で，全体の成績の底上げだけでなく，化学療法により新たに切除可能となる例や肺転移疑い例などに対する適応など，新たな効果が期待される．CPT-11+TS-1は外来投与も容易で本邦ではすでに広く用いられているが，現在国内でFORFIRIとの臨床比較試験が行われており効果に対する最終的な結論はこの結果を待ちたい．ただし現時点では，化学療法による長期CRの報告はきわめてまれで，補助療法の域を脱しておらず，長期生存を期待するには手

表2 肺転移を伴うstage IV大腸癌の検討すべき予後因子

(身体所見)	性別，年齢
(原発巣)	部位(結腸，直腸)，組織型，リンパ節転移(有無，個数)， 病期／進行度，郭清度，術前CEA，術後CEA， 原発巣術後化学療法(neoadjuvant)の有無
(肺外転移巣)	肺外遠隔(肝転移，腹膜播腫など)転移の有無
(肺転移巣)	原発巣切除から肺切除までの期間(1期的，2期的，など)， 転移個数，最大径，片側性か両側性か，末梢性か中枢性か， 転移巣組織型，肺門・縦郭リンパ節転移の有無，胸水の有無， 胸膜浸潤の有無，開胸時洗浄細胞診，胸膜播腫の有無， 肺切除術式，肺切除根治度，肺切除断端距離，輸血の有無， 肺切除前CEA，肺切除後CEA，周術期合併症の有無，在院日数， 肺切除後化学療法(adjuvant)の有無， 肺再発の有無，肺再切除の有無，肺外再発の有無，など

術と併用する必要がある．

原則的に大腸癌の肺転移は，systemic diseaseと考えられるが，局所制御にメリットがあると考えられる場合には，手術以外に以下のような局所療法が存在する．

2．ラジオ波組織熱凝固療法 (RFA：radio-frequency ablation)

肝ではなく，肺に対するFRAの報告は2002年頃より散見される．Yanらは切除不能大腸癌肺転移例に対す経皮的なRFAの成績として，1年生存85%，2年生存64%，3年生存46%(平均観察期間2年)という成績を報告しており，予後不良因子は最大転移径3 cm以上である[17]．

3．放射線療法

肺転移巣に対して，定位的，また3次元に狭い領域にビームを集光する定位的3次元集光照射(stereotactic radiation therapy，SRT)が普及してきている．治療期間の短縮(小分割化)も目的とされ，Haraらは転移性肺癌48例(うち大腸癌由来は9例)，原発性肺癌11例を対象に30 Gy前後の1回照射で，1年局所制御率93%，2年局所制御率78%と良好な成績を報告している[18]．また，より局所制御に優れているとされる重粒子線[19]も，すでに重粒子医科学センター病院や兵庫県立粒子線医療センター病院では肺転移巣に照射する試みがなされており，その結果が期待される．

おわりに

肺転移を伴うstage IV大腸癌の治療方針について検討した．当施設の切除症例数は12例と少ないが，肺単独でしかも孤立性転移の成績は良好で長期生存も得られている．また，肺肝転移例では成績が劣るものの文献的に非切除の成績と比較すると良好であり，切除可能であれば原発巣と転移巣を切除するという原則は成り立っている．今後は，多施設間の多数症例で予後規定因子を検討し良好な手術適応を決定するとともに，化学療法や放射線療法などの集学的治療を駆使して予後やQOLを改善する必要がある．

文　献

1) 大腸癌研究会編：大腸癌治療ガイドライン 医師用 2005年版，金原出版，東京，2005.
2) Thomford NR, Woolner LB, Clagett OT: The surgical treatment of metastatic tumors in the lung. J Thorac Cardiovasc Surg 49: 357-363, 1965.
3) Okumura S, Kondo H, Tsuboi M, et al: Pulmonary resection for metastatic colorectal cancer; experiences with 159 patients. J Thorac Cardiovasc Surg 112: 867-874, 1996.
4) Higashiyama M, Kodama K, Higaki N, et al: Surgery for pulmonary metastases from colorectal cancer: the importance of prethoracotomy serum carcinoembryonic antigen as an indicator of prognosis. Jpn J Thorac Crdiovasc Surg 51: 289-296, 2003.
5) Yedibela S, Klein P, Feuchter K, et al: Surgical management of pulmonary metastases from colorectal cancer in 153 patients. Annals of Surg Oncol 13: 1538-1544, 2006.
6) 金光幸秀，加藤知行，平井　孝：大腸癌肺転移に対する治療の現況－第55回大腸癌研究会アンケート結果．日本大腸肛門病会誌　57：121-131，2004.
7) Higashiyama M, Kodama K, Higaki N, et al: Surgical treatment for metastatic lung tumors with incidentally coexisting lung cancer. Jpn J Thorac Cardiovasc Surg 47: 185-189, 1999.
8) 東山聖彦，高見康二，檜垣直純ほか：大腸癌肺転移に対する外科治療．臨床消化器内科　20：199-206，2005.
9) Higashiyama M, Kodama K, Takami K, et al: Intraoperative lavage cytologic analysis of surgical margins as a predictor of local recurrence in pulmonary metastatectomy. Arch Surg 137: 467-474, 2002.
10) Regnard JF, Grunenwald D, Spaggaiari L, et al: Surgical treatment for hepatic and pulmonary metastases from colorectal cancers. Ann Thorac Surg 66: 214-218, 1998.
11) Ambiru S, Miyazaki M, Ito H, et al: Resection of hepatic and pulmonary metastases in patients with colorectal carcinoma. Cancer 82: 274-278, 1998.
12) Shah SA, Haddad R, Al-Sukhni W, et al: Surgical resection of hepatic and pulmonary metastases from colorectal carcinoma. J Am Coll Surg 202: 468-475, 2006.
13) Kandioler D, Kromer E, Tuchler H, et al: Long-term results after repeated surgical removal of pulmonary metastases. Ann Thorac Surg 65: 909-912, 1998.
14) Girard P, Ducreux M, Baldeyrou P, et al: Surgery for lung metastases from colorectal cancer: analysis of prognostic factors. J Clin Oncol 14: 2047-2053, 1997.
15) Goldberg R, Sargent D, Morton R, et al: A randomized controlled trial of fluorouracil plus leucovorin, irinotecan, and oxaliplatin combinations in patients with previously untreated metastatic colorectal cancer. J Clin Oncol 22: 23-30, 2004.
16) Tournigand C, André T, Achille E, et al: FOLFIRI followed by FOLFOX6 or the reverse sequence in

Available online at www.sciencedirect.com
ScienceDirect
Analytical Biochemistry 364 (2007) 37–50
ANALYTICAL BIOCHEMISTRY
www.elsevier.com/locate/yabio

Novel fucogangliosides found in human colon adenocarcinoma tissues by means of glycomic analysis

Hiroaki Korekane [a,b], Satoyo Tsuji [a], Shingo Noura [c], Masayuki Ohue [c], Yo Sasaki [c], Shingi Imaoka [c], Yasuhide Miyamoto [a,*]

[a] *Department of Immunology, Osaka Medical Center for Cancer and Cardiovascular Diseases, 1-3-2 Nakamichi, Higashinari-ku, Osaka 537-8511, Japan*
[b] *Japan Health Science Foundation, 13-4 Nihonbashi Kodenma-cho, Chuo-ku, Tokyo 103-0001, Japan*
[c] *Department of Surgery, Osaka Medical Center for Cancer and Cardiovascular Diseases, 1-3-3 Nakamichi, Higashinari-ku, Osaka 537-8511, Japan*

Received 29 November 2006
Available online 31 January 2007

Abstract

The structures of acidic glycosphingolipids in colon adenocarcinoma have been analyzed extensively using a number of conventional methods, such as thin-layer chromatography and methylation analysis, and a variety of acidic glycosphingolipids present in the tissues have been reported. However, because of a number of limitations in the techniques used in previous studies in terms of resolution, quantification, and sensitivity, we employed a different method that could be applied to small amounts of tissue. In this technique, the carbohydrate moieties of acidic glycosphingolipids from approximately 20 mg of colon adenocarcinoma were released by endoglycoceramidase II and were labeled by pyridylamination. They were separated and structurally characterized by a two-dimensional HPLC mapping technique, electrospray ionization tandem mass spectrometry (ESI–MS/MS), and enzymatic cleavage. A total of 22 major acidic glycosphingolipid structures were identified, and their relative quantities were revealed in detail. They are composed of 1 sulfated (SM3), 1 lacto-series (SLe^a), 6 kinds of ganglio-series, and 14 kinds of neolacto-series glycosphingolipids. They include most of the acidic glycosphingolipids previously reported to be present in the tissues and two previously unknown fucogangliosides sharing the same terminal structure: NeuAcα2-6(Fucα1-2)Galβ1-4GlcNAcβ1-3Galβ1-4Glc, and NeuAcα2-6(Fucα1-2)Galβ1-4GlcNAcβ1-3Galβ1-4(Fucα1-3)GlcNAcβ1-3-Galβ1-4Glc. Thus, this highly sensitive, high-resolution analysis enabled the identification of novel structures of acidic glycosphingolipids from small amounts of already comprehensively studied cancerous tissues. This method is a powerful tool for microanalysis of glycosphingolipid structures from small quantities of cancerous tissues and should be applicable to different types of malignant tissues.

Keywords: Ganglioside; Colon cancer; Structure; Pyridylamination; Mass spectrometry; Two-dimensional mapping

* Corresponding author. Fax: +81 6 6972 7749.
E-mail address: miyamoto-ya@mc.pref.osaka.jp (Y. Miyamoto).

0003-2697/$ - see front matter © 2007 Elsevier Inc. All rights reserved.
doi:10.1016/j.ab.2007.01.034

Alterations in glycosphingolipid (GSL)[1] compositions on the cell surface of tumors occur in essentially all types of human cancers [1]. Extensive studies have been performed to analyze the structure of GSLs from a variety of tumor tissues [2–7]. Furthermore, a series of GSLs unusually accumulated in cancerous tissues have been successfully isolated and characterized [8–11] and reveal that each type of tumor is characterized by accumulation of specific types of GSLs. For example, unusual accumulations of GSLs having type 1 or 2 chain derivatives (i.e., those with Le^a, Le^x, Le^y, or dimeric Le^x and their sialosyl derivatives) are observed in most human adenocarcinoma [9,11–13], whereas GD3 is observed in melanoma [3]. However, due to a number of limitations of the techniques used, these analyses may be lacking in terms of identification and quantification. In general, in the techniques applied previously, GSLs extracted from cancerous tissues were separated by HPLC using organic solvents and traditional thin-layer chromatography (TLC) methodology where resolved GSLs were stained with orcinol. A single band on TLC might not ensure homogeneity, and separation of GSLs having similar mobility on TLC sometimes may be difficult even though a variety of separation solvents are used [13]. Hence, it is possible that certain GSLs having similar chromatographic behavior on TLC were not separated to homogeneity and escaped detection even in well-studied cancerous tissues. Furthermore, although quantification of each GSL is important to better understand the precise features of glycosylation of cancerous tissue, the quantities of individual GSLs in cancer tissues have not been well defined because quantification by scanning densitometry of orcinol-stained bands on TLC is limited by the severe restriction in the linear range due to variation in band size or geometry following migration. Thus, more detailed analyses of GSL structures in cancerous tissues using improved methodology that overcomes the limitations described above may be required, even in tissues already well studied.

Here we employ a powerful methodology to analyze the structures of GSLs from small quantities of colon adenocarcinoma (~ 20 mg). The techniques are highly sensitive and capable of separating the major GSLs and analyzing them quantitatively as well as qualitatively [14]. The methodology employs the use of endoglycoceramidase to release the carbohydrate moieties of GSLs, fluorescent labeling with 2-aminopyridine, and HPLC analysis. Furthermore, each GSL could be identified by a two-dimensional (2-D) mapping technique together with electrospray ionization–tandem mass spectrometry (ESI–MS/MS).

Colon adenocarcinoma is one of the most widely examined tissues in terms of the structures of GSLs of cancerous tissues [2,8–13,15] and was used as the source of material in this study to allow us to evaluate the effectiveness of the new techniques through comparison with results reported previously.

In this study, we focus on the acidic GSLs among the GSLs and elucidate the fine structures of major acidic GSLs present in colonic adenocarcinoma tissues more precisely than reported previously. In particular, we describe the structure of novel fucosyl gangliosides.

Materials and methods

Isolation of acidic GSLs from colon adenocarcinoma tissues

All patients had undergone simultaneous resections of primary colon tumors and liver metastases at Osaka Medical Center for Cancer and Cardiovascular Diseases (Osaka, Japan). Fresh cancerous tissues were frozen with liquid nitrogen and stored at –80 °C until use. The samples were cut to a thickness of 10 μm with a cryostat microtome. A total of 20 sections were collected, homogenized in 10 ml of chloroform/methanol (2:1, v/v), and stored for 2 h at room temperature with 30 s of sonication every 30 min. Then 5 ml of methanol was added, and the sample was centrifuged at 1800 *g* for 15 min. The pellets were homogenized in 10 ml of chloroform/methanol/water (1:2:0.8, v/v/v), stored for 2 h at room temperature, and centrifuged at 1800 *g* for 15 min. Both extracts were combined and evaporated to dryness in a vacuum concentrator. The residue was dissolved in chloroform/methanol/water (30:60:8) and fractionated by DEAE–Sephadex A25 column chromatography into neutral and acidic GSLs.

Preparation of acidic pyridylaminated oligosaccharides

The acidic GSLs were digested at 37 °C for 16 h with 10 mU of recombinant endoglycoceramidase II from *Rhodococcus* sp. (Takara Bio, Shiga, Japan) in 50 μl of 0.1 M sodium acetate (pH 5.0) containing 0.1% taurodeoxycholate [16]. Released oligosaccharides were labeled with 2-aminopyridine (2-AP), and excess reagent was removed by phenol/chloroform extraction [17,18].

[1] *Abbreviations used:* GSL, glycosphingolipid; GD3, Neu5Acα8Neu5Acα3Galβ-4GlcCer; TLC, thin-layer chromatography; 2-D, two-dimensional; ESI–MS/MS, electrospray ionization–tandem mass spectrometry; 2-AP, 2-aminopyridine; PA, pyridylaminated; Gu, glucose units; RP, reversed phase; CID, collision-induced dissociation; asialo GM2, GalNAcβ4Galβ4Glc; asialo GM1, Galβ3GalNAcβ4Galβ4Glc; GM3, Neu5Acα3Galβ4Glc; GM2, GalNAcβ4(Neu5Acα3)Galβ4Glc; GD1a, Neu5Acα3Galβ3GalNAcβ4(Neu5Acα3)Galβ4Glc; GD1b, Galβ3GalNAcβ4(Neu5Acα8Neu5Acα3)Galβ4Glc; GT1b, Neu5Acα3Galβ3GalNAcβ4(Neu5Acα8Neu5Acα3)Galβ4Glc; GQ1b, Neu5Acα8Neu5Acα3Galβ3GalNAcβ4(Neu5Acα8Neu5Acα3)Galβ4Glc; globotriose, Galα4Galβ4Glc; Le^b-hexasaccharide, Fucα2Galβ3(Fucα4)GlcNAcβ3Galβ4Glc; A-hexasaccharide, GalNAcα3(Fucα2)Galβ3GlcNAcβ3Galβ4Glc; A-heptasaccharide, GalNAcα3(Fucα2)Galβ3(Fucα4)GlcNAcβ3Galβ4Glc; 2-fucosyllactose, Fucα2Galβ4Glc; A-tetrasaccharide, GalNAcα3(Fucα2)Galβ4Glc; SM2,GalNAcβ4(HSO^3)3Galβ4GlcCer; SM3, $HSO^3$3Galβ4GlcCer; H^1, Fucα2Galβ4GlcNAcβ3Galβ4Glc; Lc^4, Galβ3GlcNAcβ3Galβ4Glc; nLc^4, Galβ4GlcNAcβ3Galβ4Glc; Cer, ceramide; LST-c, Neu5Acα6Galβ4GlcNAcβ3Galβ4Glc; SPG, sialyl-paragloboside, Neu5Acα3Galβ4GlcNAcβ3Galβ4Glc; LST-a, Neu5Acα3Galβ3GlcNAcβ3Galβ4Glc; SLex, sialyl-Lewis X, Neu5Acα3Galβ4(Fucα3)GlcNAcβ3Galβ4GlcCer.

HPLC for pyridylaminated-oligosaccharides separation

Pyridylaminated (PA)-oligosaccharides were separated on a Shimazu LC-20A HPLC system equipped with a Waters 2475 fluorescence detector. Size fractionation HPLC was performed on a TSK gel Amide-80 column (0.2 × 25 cm, Tosoh, Tokyo, Japan) at 40 °C at a flow rate of 0.2 ml/min using two solvents: A and B. Solvent A was acetonitrile/0.5 M acetic acid containing 10% acetonitrile, adjusted to pH 7.3 with triethylamine (75:15, v/v). Solvent B was acetonitrile/0.5 M acetic acid containing 10% acetonitrile, adjusted to pH 7.3 with triethylamine (40:50, v/v). The column was equilibrated with solvent A. After injection of sample, the proportion of solvent B was programmed to increase from 0 to 100% in 100 min. The PA-oligosaccharides were detected by fluorescence with an excitation wavelength of 310 nm and an emission wavelength of 380 nm. The molecular size of each PA-oligosaccharide is given in glucose units (Gu) based on the elution times of PA-isomaltooligosaccharides. Reversed phase (RP)–HPLC was performed on a TSK gel ODS-80Ts column (0.2×15 cm, Tosoh) at 30 °C at a flow rate of 0.2 ml/min using two solvents: C and D. Solvent C was 50 mM acetic acid, adjusted to pH 6.0 with triethylamine. Solvent D was 50 mM acetic acid containing 20% acetonitrile, adjusted to pH 6.0 with triethylamine. The column was equilibrated with solvent C. After injection of sample, the proportion of solvent D was programmed to increase from 0 to 18% in 54 min. The PA-oligosaccharides were detected by excitation at 315 nm and emission at 400 nm. The retention time of each PA-oligosaccharide is given in glucose units based on the elution times of PA-isomaltooligosaccharides. Thus, a given compound from these two columns provided a unique set of Gu (amide) and Gu (ODS) values that correspond to coordinates of the 2-D map. When coordinates are cited in this article, they are listed in the order of Gu (ODS), Gu (amide).

Glycosidase digestion

Sialyl PA-oligosaccharides were digested with 2 U/ml of α2,3-sialidase from *Salmonella typhimurium* (Takara Bio) or 2 U/ml α-sialidase from *Arthrobacter ureafaciens* (Nacalai, Kyoto, Japan) in 100 mM sodium acetate buffer (pH 5.5) for 2 h at 37 °C (condition 1). Under these conditions, α2,3-sialidase specifically digests sialic acid α2-3 linked to the terminal residue but not sialic acid with a α2-6 linkage, whereas *Arthrobacter* α-sialidase digests both linkages independent of the linkage position. However, under conditions using 10 U/ml for 16 h (condition 2), even so-called α2,3-sialidase can hydrolyze sialic acid α2-6 linked to the terminal residue but not sialic acid linked to a nonterminal residue. Hence, we were able to conclude the linkage position of sialic acid using these two enzymes as follows. First, when sialyl PA-oligosaccharide was cleaved by α2,3-sialidase in condition 1, sialic acid was concluded to be linked to the terminal residue through an α2-3 linkage. Second, when sialyl PA-oligosaccharide was cleaved by α2,3-sialidase in condition 2 but not in condition 1, sialic acid was concluded to be linked to the terminal residue through an α2-6 linkage. Third, when sialyl PA-oligosaccharide was cleaved by *Arthrobacter* α-sialidase in condition 1 but not by α2,3-sialidase even in condition 2, sialic acid was concluded to be linked to a nonterminal residue. The enzyme specificity was demonstrated using the following model substrates: NeuAcα2-3Galβ1-4GlcNAcβ1-3Galβ1-4Glc-PA (sialylparagloboside), NeuAcα2-6Galβ1-4GlcNAcβ1-3Galβ1-4Glc-PA (LS-tetrasaccharide *c*), Galβ1-3(NeuAcα2-6)GlcNAcβ1-3Galβ1-4Glc-PA (LS-tetrasaccharide *b*), and Galβ1-3GalNAcβ1-4(NeuAcα2-3)Galβ1-4Glc-PA (GM1).

In other glycosidase digests, PA-oligosaccharides were digested with (i) 0.2 mU/ml of α1,3/4-fucosidase from *Streptomyces* sp. 142 (Takara Bio) in 100 mM sodium acetate buffer (pH 5.5) for 2 h at 37 °C, (ii) 0.4 U/ml β1,4-galactosidase from *Streptococcus pneumonia* (Prozyme, San Leandro, CA, USA) in 100 mM sodium citrate buffer (pH 6.0) for 2 h at 37 °C, (iii) 10 U/ml of β-*N*-acetylhexosaminidase from jack bean (Seikagaku Kogyo, Tokyo, Japan) in 100 mM sodium citrate buffer (pH 5.0) for 16 h at 37 °C, (iv) 4 U/ml of α1,2-fucosidase from *Corynebacterium* sp. (Takara Bio) in 100 mM sodium phosphate buffer (pH 8.5), (v) 0.5 U/ml of endo-β-galactosidase from *Escherichia freundii* (Seikagaku Kogyo) in 100 mM sodium acetate buffer (pH 5.8) for 16 h at 37 °C, and (vi) 10 U/ml of α-fucosidase from bovine kidney (Sigma, St. Louis, MO, USA) in 100 mM sodium acetate buffer (pH 5.8) for 16 h at 37 °C. All of the reactions were terminated by boiling the solutions for 3 min at 100 °C.

Electrospray ionization MS^n

PA-oligosaccharides were analyzed by LC/ESI–MS/MS. HPLC was performed on a Paradigm MS4 equipped with a Magic C18 column (0.2 × 50 mm, Michrome BioResource, Auburn, CA, USA). Each PA-oligosaccharide was injected with a flow rate of 2 μl/min for 3 min and eluted with 50% methanol for 10 min.

MS analyses were performed using an LCQ ion trap mass spectrometer (Thermo Finnigan, San Jose, CA, USA) equipped with a nano-electrospray ion source (AMR, Tokyo, Japan). The nanospray voltage was set to 1.8 kV in the positive ion mode. The heated desolvation capillary temperature was set to 180 °C. In the LCQ method file, the LCQ was set to acquire a full MS scan between *m/z* 400 and 2000 followed by MS/MS or MS/MS/MS scans in a data-dependent manner. Relative collision energy for collision-induced dissociation (CID) was set to 30% with a 30-ms activation time for MS^2 and MS^3 experiments. MS^2 and MS^3 were performed with an isolation width of 4.0 u (range of precursor ion ± 2.0). Protonated ions were subjected to a further product ion scan for nonfucosylated PA-oligosaccharides. However, sodiated ions were subjected to a further product ion scan for

fucose-containing PA-oligosaccharides because intramolecular fucose rearrangements have been found in the CID spectra of protonated ions (but not in sodiated ions) produced from oligosaccharides derivatized at their reducing termini with aromatic amines, such as 2-aminobenzamide, which may lead to erroneous conclusions about oligosaccharide sequence [19].

Standard PA-oligosaccharides

Standard PA-oligosaccharides, including PA-lactose, PA-asialo GM2, PA-asialo GM1, PA-GM3, PA-GM2, PA-GM1, PA-GD1a, PA-GD1 b, PA-GD3, PA-GT1b, PA-GQ1b, PA-globotriose, PA-globotetraose, PA-Forssman pentsaccharide, PA-lactoneotetraose, PA-lactotetraose, PA-lactofucopentaose I, PA-lactofucopentaose II, PA-lactofucopentaose III, PA-Le^b-hexasaccharide, PA-A-hexasaccharide, PA-A-heptasaccharide, PA-2-fucosyllactose, and PA-A-tetrasaccharide, were purchased from Takara Bio. Glycolipids SM2 and SM3 were kindly donated by Koichi Honke (Kochi University Medical School). Sialylated Le^x glycolipid was purchased from Wako Pure Chemicals (Tokyo, Japan). Oligosaccharides, including LS-tetrasaccharide *a*, LS-tetrasaccharide *b*, and LS-tetrasaccharide *c*, were purchased from Prozyme, and Lewis Y hexasaccharide was purchased from Sigma. SM3, SM2, sialylated Le^x, LS-tetrasaccharide *a*, LS-tetrasaccharide *b*, LS-tetrasaccharide *c*, and Lewis Y hexasaccharide were pyridylaminated as described above. PA-H_1 was obtained from PA-Lewis Y hexasaccharide by releasing the fucosyl residue linked to the third GlcNAc by α1,3/4-fucosidase digestion. PA-sialylparagloboside was prepared from human erythrocytes using the following procedure. Acidic GSLs were extracted from 3 ml of human erythrocytes, pyridylaminated, and resolved by size fractionation HPLC as described above. Sialylparagloboside was most abundant in acidic GSLs of erythrocytes. Fractions corresponding to PA-sialylparagloboside were collected and further purified by RP–HPLC. The structure of PA-sialylparagloboside was unambiguously confirmed by enzymatic digestion and MS. GlcNAcβ1-3Galβ1-4Glc-PA and GlcNAcβ1-3Galβ1-4GlcNAcβ1-3Galβ1-4Glc-PA were prepared as standard compounds for endo-β-galactosidase treatment by digestion of PA-nLc_4 and PA-nLc_6, respectively, with β1,4-galactosidase (see Results). Although 2-D mapping techniques have been widely used for the analysis of structures of *N*-glycans, the technique seldom has been applied to the analysis of structures of GSLs. Hence, prior to analysis of cancerous tissues, we evaluated the potential of the method by analyzing all of the PA-oligosaccharides prepared in this study, including 16 acidic and 18 neutral oligosaccharides, by HPLC using the two types of column (ODS and amide). All of the PA-oligosaccharides except PA-lactofucopentaose II (Le^a) and PA-lactofucopentaose III (Le^x) were clearly separated on the map under the chromatographic conditions used in this study (data not shown). PA-Le^a and PA-Le^x could be discriminated following α1,3/4-fucosidase digestion because the digestion products, namely PA-lactotetraose (Lc_4) and PA-lactoneotetraose (nLc_4), elute at positions with distinct glucose units on both columns (Table 1). Hence, we concluded that the 2-D mapping technique was also applicable for the analysis of structures of GSLs. The structures, abbreviations, and glucose units of authentic PA-oligosaccharides used in this study are listed in Table 1.

Results

Preparation and separation of acidic PA-oligosaccharides from colon adenocarcinoma

Acidic GSLs from three cases of primary colonic adenocarcinoma and hepatic metastasis were extracted. Acidic glycans from the ceramide (Cer) moieties were released by endoglycoceramidase II treatment. Efficiency of release of glycans from the ceramide moiety by endoglycoceramidase II has been reported to be greater than 95% [20]. To detect sugars with high sensitivity, the reducing ends of the released oligosaccharides were tagged with the fluorophore 2-AP. Qualitatively similar, but quantitatively slightly different, chromatographic profiles of acidic PA-oligosaccharides were obtained from six samples: the primary colon cancer and liver metastatic deposits from three patients. In this article, we show the most representative data from the liver metastatic deposit of one particular patient. The acidic PA-oligosaccharides from a liver metastatic deposit of a colon adenocarcinoma were analyzed by size fractionation HPLC in which separation depends on the molecular size of the oligosaccharides (Fig. 1). A total of 17 peaks (G1–G17) were obtained (Fig. 1), with each peak being further purified by RP–HPLC. Peaks G10, G14, and G17 were separated into two major components, and G16 was separated into three major components, each designated G10-1, G10-2, G14-1, G14-2, G16-1, G16-2, G16-3, G17-1, and G17-2, in RP–HPLC. In addition, purified acidic PA-oligosaccharides were subjected to LC/ESI–MS/MS, where product ion spectra of the precursor ions were acquired data-dependently. Peaks marked by an open arrowhead in Fig. 1 contained neutral PA-oligosaccharides, as determined by MS analyses. This probably is due to desialylation of PA-oligosaccharides during the process of pyridylamination. Elution positions of G1 to G17-2 on size fractionation and RP–HPLC are summarized in Fig. 2 as a 2-D map.

Structure of G1 to G9

From comparison of the positions on the map with the positions of standard acidic PA-oligosaccharides, G1, G2, G3, G4, G5, G7, G8 and G9 are predicted to be SM3, GM3, GM2, GD3, GM1, GD1a, LST-c, and GD1b, respectively. Strong candidates for the identity of G6 are

Table 1
Structures and elution positions in HPLC of standard PA-oligosaccharides

Abbreviation	Structure	Elution position in HPLC	
		Size (Gu)	RP (Gu)
SM3	HSO_3-Galβ1-4Glc-PA	1.19	2.60
GM3	Neu5Acα2-3Galβ1-4Glc-PA	2.46	3.00
GM2	GalNAcβ1-4Galβ1-4Glc-PA 3 Neu5Acα2	2.97	3.01
GM1	Galβ1-3GalNAcβ1-4Galβ1-4Glc-PA 3 Neu5Acα2	3.85	2.92
GD3	Neu5Acα2-8Neu5Acα2-3Galβ1-4Glc-PA	3.31	4.50
GD1a	Galβ1-3GalNAcβ1-4Galβ1-4Glc-PA 3 3 Neu5Acα2 Neu5Acα2	4.10	5.03
GD1b	Galβ1-3GalNAcβ1-4Galβ1-4Glc-PA 3 Neu5Acα2-8Neu5Acα2	4.64	3.96
SPG	Neu5Acα2-3Galβ1-4GlcNAcβ1-3Galβ1-4Glc-PA	4.02	4.52
LST-a	Neu5Acα2-3Galβ1-3GlcNAcβ1-3Galβ1-4Glc-PA	4.01	4.69
LST-c	Neu5Acα2-6Galβ1-4GlcNAcβ1-3Galβ1-4Glc-PA	4.40	3.76
SLe^x	Neu5Acα2-3Galβ1-4GlcNAcβ1-3Galβ1-4Glc-PA 3 Fucα1	4.75	4.08
Lc_4	Galβ1-3GlcNAcβ1-3Galβ1-4Glc-PA	3.66	2.50
nLc_4	Galβ1-4GlcNAcβ1-3Galβ1-4Glc-PA	3.74	2.16
H_1	Fucα1-2Galβ1-4GlcNAcβ1-3Galβ1-4Glc-PA	4.15	3.80
LFP II (Le^a)	Galβ1-3GlcNAcβ1-3Galβ1-4Glc-PA 4 Fucα1	4.51	2.01
LFP III (Le^x)	Galβ1-4GlcNAcβ1-3Galβ1-4Glc-PA 3 Fucα1	4.51	1.99

SPG and LST-a (Fig. 2). After α2,3-sialidase digestion, G6 was converted to nLc_4 but not Lc_4, indicating that G6 is SPG. The structures of G1 to G9 were also confirmed by MS/MS. Fractions eluting later than G9 on the amide column, with the exception of G10-1, do not match any of the reference compounds on the 2-D map (Fig. 2). In the following sections, the structures of acidic PA-oligosaccharides with the same monosaccharide compositions are explained in detail. Elution positions, mass data, and estimated composition of G10-1 to G17-2 are presented in Table 2.

Structure of G10-1, G10-2, and G11

G10-1 and G11 were digested with α2,3-sialidase in conditions in which this enzyme specifically cleaves the α2,3 linkage (condition 1). The products of both digests corresponded to either Le^a or Le^x on the map (thick-line and thin-line arrows in Fig. 3). The desialylated products from G10-1 and G11 were digested with α1,3/4-fucosidase, and the positions of the products of the digests corresponded to nLc_4 and Lc_4, respectively. These results suggest that the structure of G10-1 is SLe^x and the structure of G11 is

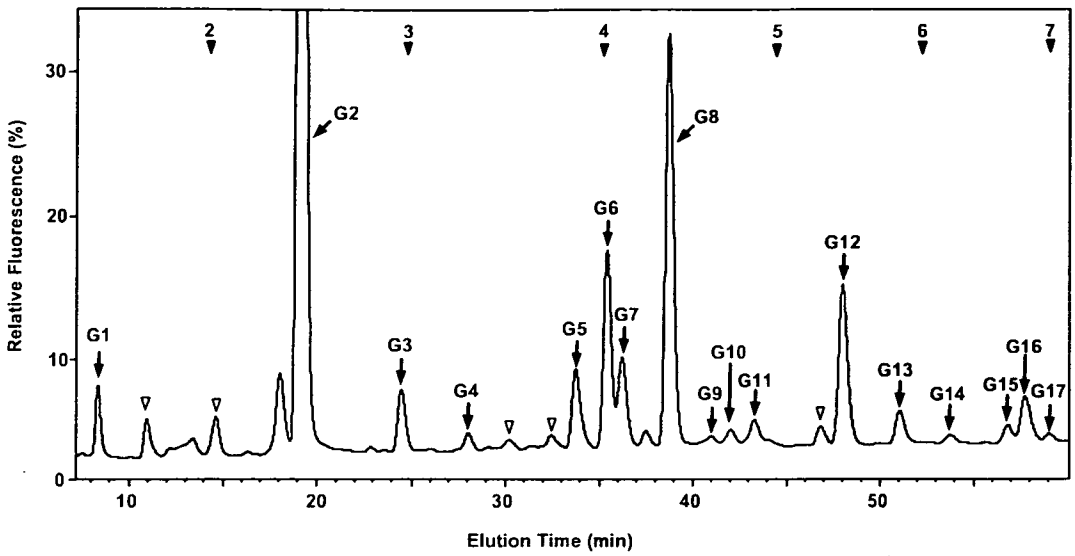

Fig. 1. Elution profile of the acidic PA-oligosaccharide mixtures obtained from colon adenocarcinoma tissue on the amide column. Relative fluorescence of the highest peak, G2, was set to 100%. A total of 17 peaks, which are predicted to be acidic PA-oligosaccharides by MS analysis, are termed G1 to G17 and highlighted with arrows. Numbered closed arrowheads indicate the elution positions of PA-isomaltooligosaccharides with the corresponding degree of polymerization. The peaks marked by the open arrowheads contained neutral PA-oligosaccharides.

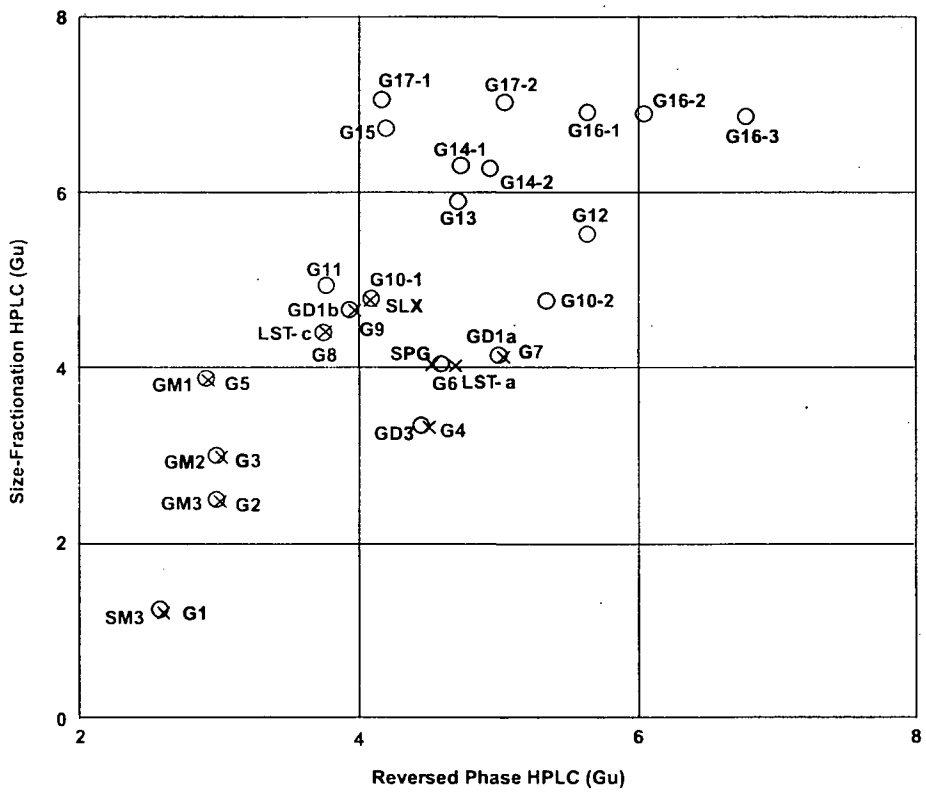

Fig. 2. Two-dimensional map of acidic PA-oligosaccharides. The elution positions of each acidic PA-oligosaccharide on the size fractionation and RP–HPLC are expressed in glucose units based on the elution times of the PA-isomaltooligosaccharides and plotted on the map. Circles indicate the positions of the acidic PA-oligosaccharides from colon adenocarcinoma tissue. Xs indicate the positions of the standard acidic PA-oligosaccharides.

SLe^a (Table 3). These structures are consistent with the structures deduced by MS/MS analysis (Fig. 4, right, with only MS$^{1-3}$ spectra of G11 shown in the figure). In contrast to G10-1 and G11, G10-2 could not be digested with α2,3-sialidase in the conditions where this enzyme specifically cleaves the α2-3 linkage (condition 1) but could be digested with α2,3-sialidase in the conditions where this enzyme cleaves the α2-3 and α2-6 linkages (condition 2). These

Table 2
Elution positions in HPLC and mass analysis of acidic PA-oligosaccharides from colon adenocarcinoma tissue eluted later than G9 on the amide column

Fraction	Elution position in HPLC		Mass (observed)	Mass (calculated)	Estimated composition
	Size (Gu)	RP (Gu)			
G10-1	4.78	4.09	1223.5	1223.5 $[M+H]^+$	$NeuAc_1Hex_3HexNAc_1dHex_1$-PA
G10-2	4.74	5.35	1223.5	1223.5 $[M+H]^+$	$NeuAc_1Hex_3HexNAc_1dHex_1$-PA
G11	4.92	3.77	1223.3	1223.5 $[M+H]^+$	$NeuAc_1Hex_3HexNAc_1dHex_1$-PA
G12	5.51	5.64	1442.4	1442.5 $[M+H]^+$	$NeuAc_1Hex_4HexNAc_2$-PA
G13	5.89	4.71	1442.6	1442.5 $[M+H]^+$	$NeuAc_1Hex_4HexNAc_2$-PA
G14-1	6.29	4.73	1588.4	1588.6 $[M+H]^+$	$NeuAc_1Hex_4HexNAc_2dHex_1$-PA
G14-2	6.25	4.94	1588.3	1588.6 $[M+H]^+$	$NeuAc_1Hex_4HexNAc_2dHex_1$-PA
G15	6.71	4.19	1588.4	1588.6 $[M+H]^+$	$NeuAc_1Hex_4HexNAc_2dHex_1$-PA
G16-1	6.90	5.64	1807.1	1807.7 $[M+H]^+$	$NeuAc_1Hex_5HexNAc_3$-PA
G16-2	6.87	6.05	1807.4	1807.7 $[M+H]^+$	$NeuAc_1Hex_5HexNAc_3$-PA
G16-3	6.85	6.78	1807.5	1807.7 $[M+H]^+$	$NeuAc_1Hex_5HexNAc_3$-PA
G17-1	7.04	4.16	1734.4	1734.7 $[M+H]^+$	$NeuAc_1Hex_4HexNAc_2dHex_2$-PA
G17-2	7.00	5.04	1734.3	1734.7 $[M+H]^+$	$NeuAc_1Hex_4HexNAc_2dHex_2$-PA

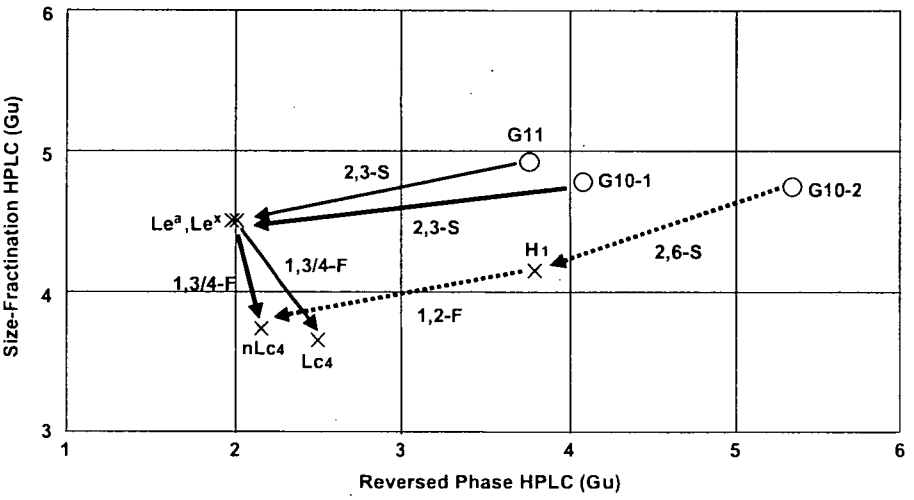

Fig. 3. Sequential digestion of PA-oligosaccharides G10-1, G10-2, and G11. Circles indicate the positions of G10-1, G10-2, and G11. Thick-line, dotted-line, and thin-line arrows indicate the directions of the changes after glycosidase digestion of G10-1, G10-2, and G11, respectively. Glycosidases are shown beside each line. Enzyme abbreviations: 2,3-S, α2,3-sialidase under conditions where the enzyme specifically digests sialic acid in the α2-3 linkage; 2,6-S, α2,3-sialidase under conditions where the enzyme digests sialic acid in both α2-3 and α2-6 linkages; 1,3/4-F, α1,3/4-fucosidase; 1,2-F, α1,2 fucosidase. Xs mark the positions of the standard compounds.

results suggest that sialic acid is α2-6 linked to the terminal residue (see Materials and Methods). In addition, the desialylated product of G10-2 corresponded to H_1 on the 2-D map (dashed-line arrows in Fig. 3). After desialylation, G10-2 could be digested with α1,2-fucosidase but not with α1,3/4-fucosidase, and the position of the product of the digest on the map corresponded with that of nLc_4. On the basis of these data, G10-2 is estimated to be NeuAcα2-6(Fucα1-2)Galβ1-4GlcNAcβ1-3Galβ1-4Glc, a structure that has not been reported previously (Table 3). These structures are consistent with the results from MS/MS analysis (Fig. 4, left). The mass spectrum of MS^3 of G10-2 revealed it to have a core tetrasaccharide structure: Hex-HexNAc-Hex-Hex-PA. The presence of a fragment ion at *m/z* 534, corresponding to $[dHex+Hex-HexNAc+Na]^+$ in the MS^3 spectra of G10-2, indicates that a fucosyl residue is linked to the outermost Hex or HexNAc residue. However, the characteristic product ion at *m/z* 792, corresponding to $[dHex-HexNAc-Hex-Hex-PA+Na]^+$, was observed in the MS^3 spectrum of G10-1 and G11 (Fig. 4, right) but not in the MS^3 spectra of G10-2, suggesting that a fucosyl residue is linked to the outermost Hex residue but not the HexNAc residue in G10-2.

Structure of G12 and G13

G12 was digested successfully with α2,3-sialidase in condition 1. In contrast, G13 could not be digested with α2,3-sialidase under the same conditions, but could be digested in condition 2. Both desialylation products had very similar behavior on the HPLC eluting at the same positions (2.93, 5.38), indicating that G12 and G13 have the same structural backbone and that sialic acid is linked α2-3 and α2-6, respectively, to the terminal residue. Desialylated products from G12 and G13 were sequentially digested

Table 3
Estimated structures of acidic PA-oligosaccharides from colonic adenocarcinoma

Fraction	Structure	Abbreviation	Ratio (%)
G1	HSO_3-Galβ1-4Glc-PA	SM3	1.6
G2	Neu5Acα2-3Galβ1-4Glc-PA	GM3	58.0
G3	GalNAcβ1-4Galβ1-4Glc-PA 3 Neu5Acα2	GM2	1.9
G4	Neu5Acα2-8Neu5Acα2-3Galβ1-4Glc-PA	GD3	0.6
G5	Galβ1-3GalNAcβ1-4Galβ1-4Glc-PA 3 Neu5Acα2	GM1	2.8
G6	Neu5Acα2-3Galβ1-4GlcNAcβ1-3Galβ1-4Glc-PA	SPG	6.5
G7	Galβ1-3GalNAcβ1-4Galβ1-4Glc-PA 3 3 Neu5Acα2 Neu5Acα2	GD1a	2.9
G8	Neu5Acα2-6Galβ1-4GlcNAcβ1-3Galβ1-4Glc-PA	IV ^{6}NeuAcα-nLc$_4$	13.8
G9	Galβ1-3GalNAcβ1-4Galβ1-4Glc-PA 3 Neu5Acα2-8Neu5Acα2	GD1b	0.2
G10-1	Neu5Acα2-3Galβ1-4GlcNAcβ1-3Galβ1-4Glc-PA 3 Fucα1	SLe^x	0.4
G10-2	Neu5Acα2-6Galβ1-4GlcNAcβ1-3Galβ1-4Glc-PA 2 Fucα1	IV^{2}Fucα,IV^{6}NeuAcα-nLc$_4$	0.2
G11	Neu5Acα2-3Galβ1-3GlcNAcβ1-3Galβ1-4Glc-PA 4 Fucα1	SLe^a	1.3
G12	Neu5Acα2-3Galβ1-4GlcNAcβ1-3Galβ1-4GlcNAcβ1-3Galβ1-4Glc-PA	VI^{3}NeuAcα-nLc$_6$	6.0
G13	Neu5Acα2-6Galβ1-4GlcNAcβ1-3Galβ1-4GlcNAcβ1-3Galβ1-4Glc-PA	VI^{6}NeuAcα-nLc$_6$	1.2
G14-1	Neu5Acα2-3Galβ1-4GlcNAcβ1-3Galβ1-4GlcNAcβ1-3Galβ1-4Glc-PA 3 Fucα1	VI^{3}NeuAcα,III^{3}Fucα-nLc$_6$	0.1
G14-2	Neu5Acα2-3Galβ1-4GlcNAcβ1-3Galβ1-4GlcNAcβ1-3Galβ1-4Glc-PA 3 Fucα1	VI^{3}NeuAcα,V^{3}Fucα-nLc$_6$	0.1
G15	Neu5Acα2-6Galβ1-4GlcNAcβ1-3Galβ1-4GlcNAcβ1-3Galβ1-4Glc-PA 3 Fucα1	VI^{6}NeuAcα,III^{3}Fucα-nLc$_6$	0.7
G16-1	Neu5Acα2-3Galβ1-4HexNAc Galβ1-4GlcNAcβ1-3Galβ1-4Glc-PA 3 Galβ1-4GlcNAcβ1		0.1
G16-2	Galβ1-4HexNAc Galβ1-4GlcNAcβ1-3Galβ1-4Glc-PA 3 Neu5Acα2-3Galβ1-4GlcNAcβ1		0.2
G16-3	Neu5Acα2-3Galβ1-4GlcNAcβ1-(3Galβ1-4GlcNAcβ1)$_2$-3Galβ1-4Glc-PA	VIII^{3}NeuAcα-nLc$_8$	1.0
G17-1	Neu5Acα2-3Galβ1-4GlcNAcβ1-3Galβ1-4GlcNAcβ1-3Galβ1-4Glc-PA 3 3 Fucα1 Fucα1	VI^{3}NeuAcα,V^{3}Fucα,III^{3}Fucα-nLc$_6$	0.2
G17-2	Neu5Acα2-6Galβ1-4GlcNAcβ1-3Galβ1-4GlcNAcβ1-3Galβ1-4Glc-PA 2 3 Fucα1 Fucα1	VI^{2}Fucα,VI^{6}NeuAcα,III^{3}Fucα-nLc$_6$	0.1

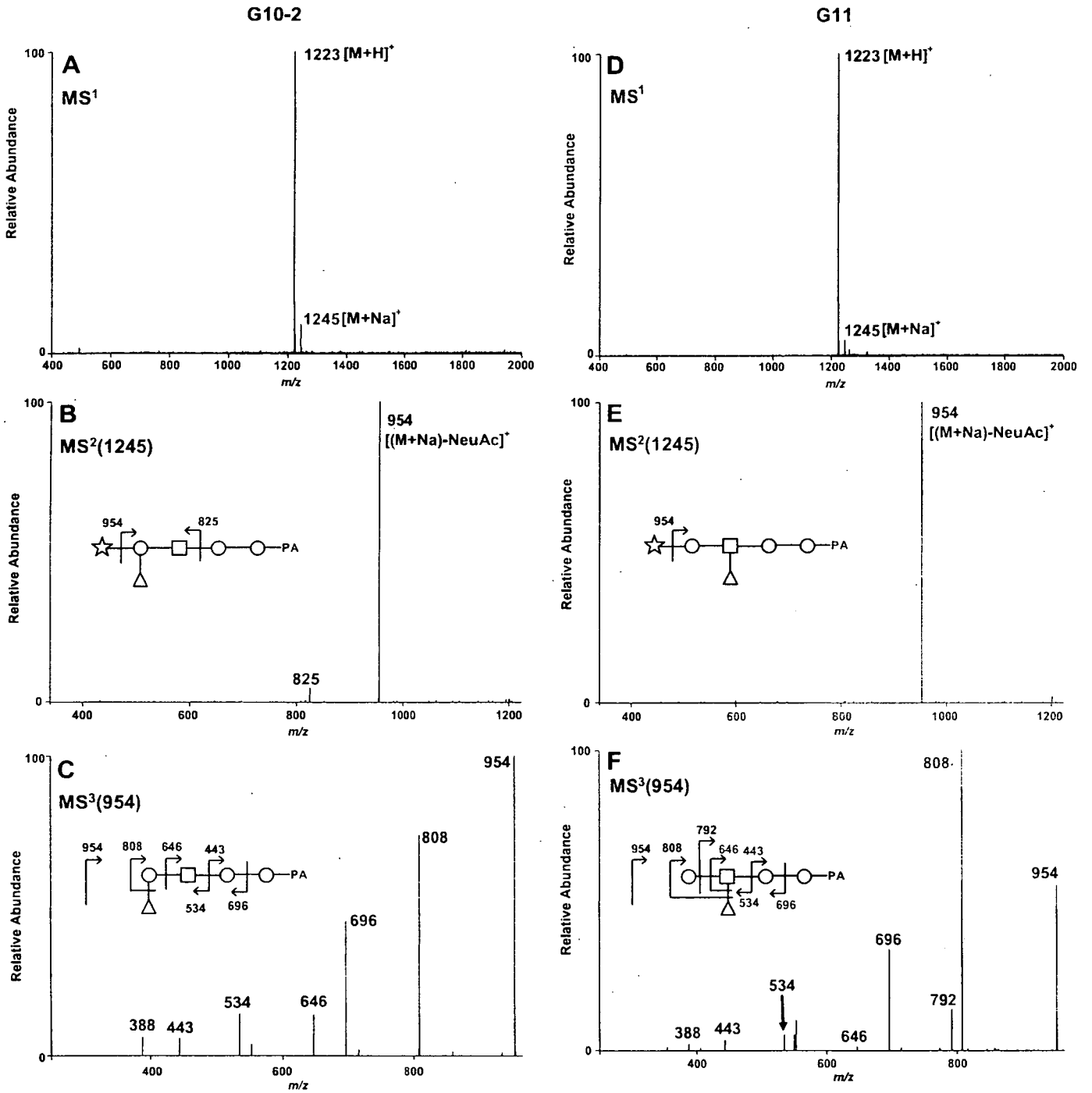

Fig. 4. MS^{1-3} spectra of G10-2 and G11. (A,D) MS^1 spectra of G10-2 (A) and G11 (D). (B,E) MS^2 spectra of $[M+Na]^+$ precursor ion at m/z 1245 detected in MS^1 of panel A (B) and panel D (E). (C,F) MS^3 spectra of $[(M+Na)\text{-NeuAc}]^+$ precursor ion at m/z 954 detected in MS^2 of panel B (C) and panel E (F). Fragment ions numbered mass values in panels B, C, E, and F are sodium adduct ions. The MS/MS fragment ions were assigned as shown schematically. Symbols: open circle, Hex; open square, HexNAc; open star, sialic acid; open triangle, dHex.

with β1,4-galactosidase and β-*N*-acetylhexosaminidase. The products of both digests corresponded to nLc_4 on the map, indicating the structure of both backbones to be Galβ1-4HexNAc-Galβ1-4GlcNAcβ1-3Galβ1-4Glc. Hydrolysis of G12 and G13 with endo-β-galactosidase gave two peaks by HPLC, corresponding Glc-PA and GlcNAcβ1-3Galβ1-4Glc-PA. These results indicate that the subterminal HexNAc is GlcNAc linked β1-3 to galactose. Hence, the structures of G12 and G13 are estimated to be as shown in Table 3. These structures are consistent with tandem mass analysis data (data not shown).

Structure of G14-1, G14-2, and G15

Sialic acid is linked α2-3 to the terminal residue of G14-1 and G14-2 and linked α2-6 to terminal residue

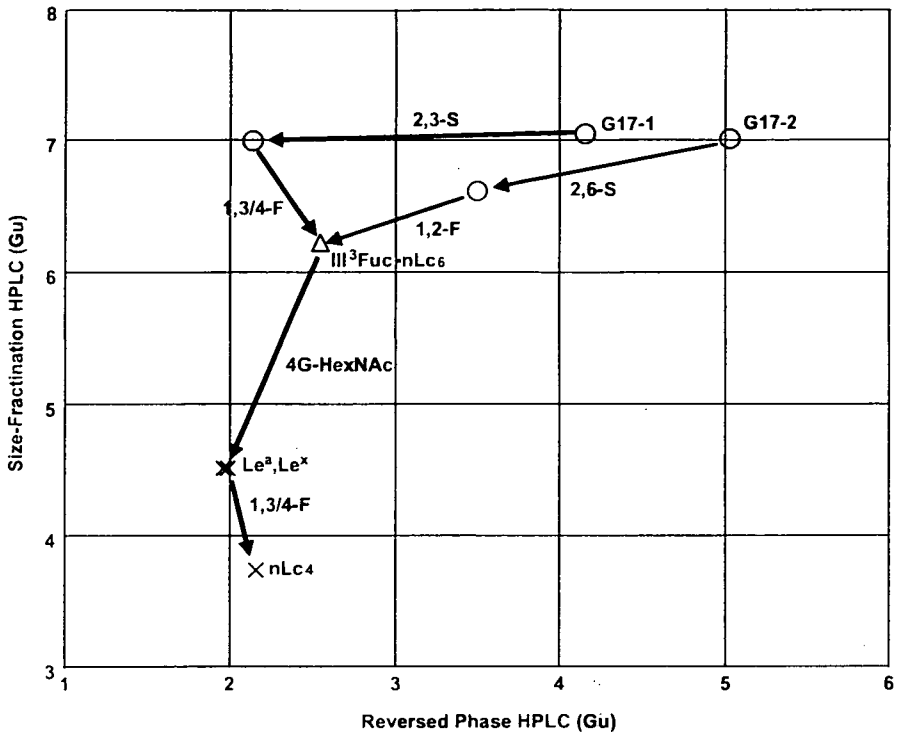

Fig. 5. Sequential digestion of PA-glycans G17-1 and G17-2. Circles indicate the positions of G17-1, G17-2, and their digests. Thick-line and thin-line arrows indicate the directions of the changes after glycosidase digestion of G17-1 and G17-2, respectively. Glycosidases are shown beside each line. Enzyme abbreviations and Xs are the same as in Fig. 3. The triangle represents the reference compound, III^{3}Fuc-nLc6, which was obtained in the analysis of the structure of G14-1 and G15.

of G15, as determined by α2,3-sialidase digestion as described above. After sialidase digestion, G14-1 and G15 had the same elution position (2.51, 6.23), whereas the coordinates of the desialylated product of G14-2 were (2.49, 6.12). These results indicate that the desialylated structures of G14-1 and G15 are the same but are different from desialylated G14-2. After sequential digestion with β1,4-galactosidase, β-*N*-acetylhexosaminidase and α1,3/4-fucosidase, the digestion products of G15 changed into the reference compound nLc$_4$. From these results, the structure of G15 is tentatively predicted to be NeuAcα2-6Galβ1-4HexNAc-Galβ1-4(Fucα1-3)GlcNAcβ1-3Galβ1-4Glc. After the fucosyl residue linked to the proximal GlcNAc of G15 was digested with bovine kidney fucosidase, the defucosylated product of G15 was cleaved by endo-β-galactosidase. The products of the digestion showed two peaks by HPLC, corresponding to Glc-PA and GlcNAcβ1-3Galβ1-4Glc-PA. The estimated structures of G15 and G14-1 are presented in Table 3. On α1,3/4-fucosidase digestion, the coordinates of desialylated G14-2 coincided with those of Galβ1-4GlcNAcβ1-3Galβ1-4GlcNAcβ1-3Galβ1-4Glc (nLc$_6$), as was determined in the above experiment, suggesting the structure of G14-2 to be NeuAcα2-3Galβ1-4(Fucα1-3)GlcNAcβ1-3Galβ1-4GlcNAcβ1-3Galβ1-4Glc (Table 3). These structures are consistent with MS/MS analysis data (data not shown).

Structure of G16-1, G16-2, and G16-3

Sialic acid is linked α2-3 to the terminal residue of G16-1, G16-2, and G16-3, as determined by α2,3-sialidase digestion. After sialidase digestion, G16-1 and G16-2 were converted to species with the same coordinates (3.66, 6.88) and G16-3 was converted to a species with coordinates (4.20, 6.88). These results indicate that G16-1 and G16-2 have the same backbone structure, which is different from that of G16-3. Desialylated G16-3 was sequentially digested with β1,4-galactosidase and β-*N*-acetylhexosaminidase twice. The first and second sequential digests gave products that corresponded to nLc$_6$ and nLc$_4$, respectively. This result indicated the structure of G16-3 to be NeuAcα2-3Galβ1-4HexNAc-Galβ1-4GlcNAcβ1-3Galβ1-4GlcNAcβ1-3Galβ1-4Glc. Endo-β-galactosidase treatment of G16-3 produced two major peaks by HPLC, corresponding to GlcNAcβ1-3Galβ1-4Glc-PA and GlcNAcβ1-3Galβ1-4GlcNAcβ1-3Galβ1-4Glc-PA. These results indicate that the subterminal HexNAc is GlcNAc linked β1-3 to galactose. On the basis of these results, the structure of G16-3 is estimated to be as listed in Table 3.

Sequential digestion of desialylated G16-2 with β1,4-galactosidase and then β-*N*-acetylhexosaminidase released two galactose and two HexNAc residues, respectively, as measured by MS (data not shown). The products of these digests coincided with the position of the reference com-